Hindawi
Advances in Meteorology
Volume 2018, Article ID 1634578, 12 pages
https://doi.org/10.1155/2018/1634578

Research Article

Investigation of the Air Pollution Event in Beijing-Tianjin-Hebei Region in December 2016 Using WRF-Chem

Dongdong Wang,[1] Baolin Jiang,[1] Fangzhou Li,[1] and Wenshi Lin[1,2]

[1]*School of Atmospheric Sciences, Sun Yat-sen University, Xingang West Road 135, Guangzhou 510275, China*
[2]*Guangdong Province Key Laboratory for Climate Change and Natural Disaster Studies, Sun Yat-sen University, Guangzhou 510275, China*

Correspondence should be addressed to Baolin Jiang; jiangblin@mail.sysu.edu.cn and Wenshi Lin; linwenshi@mail.sysu.edu.cn

Received 25 March 2018; Revised 1 June 2018; Accepted 11 June 2018; Published 31 July 2018

Academic Editor: Pedro Jiménez-Guerrero

The online coupled weather research and forecasting model with chemistry (WRF-Chem) was used to investigate an air pollution event during December 2016 in Beijing-Tianjin-Hebei urban agglomeration. Evaluation indicates that WRF-Chem captured the main weather conditions and pollutant distribution in this event. The primary meteorological drivers of air pollution formation were stationary atmospheric flows in both vertical and horizontal directions. High relative humidity and a strong temperature inversion accelerated event formation. In the shallow temperature inversion layer, aerosol particles were strongly confined near the surface, producing high surface contaminant concentrations. In addition, based on a normal experiment, three sensitivity experiments were constructed by adding hypothetical terrain (HT) of 400, 300, and 200 meters, over the region 115°E, 38.8°N to 117.54°E, 38.8°N. The results indicate that pollutants were diffused and transported below 400 meters, and the pollutant amounts concentrated south of the HT because of the HT blocking effect. Nevertheless, because there were less total contaminants north of the HT in the normal run, there was a slight decrease in pollutants north of the HT. There were some increases in pollution north of the HT because of local emissions, which were obstructed by the HT. The higher the HT, the stronger the blocking effect.

1. Introduction

Beijing-Tianjin-Hebei (BTH) is a super urban agglomeration on the North China Plain, with an area of 21,600 kilometers and more than 100 million people [1]. BTH has become one of the most heavily polluted areas in the world because of extensive industrialization and urbanization in the past few decades [2, 3]. High concentrations of fine particulates ($PM_{2.5}$, with aerodynamic diameters not larger than 2.5 μm) substantially reduce visibility through scattering, and they penetrate the human respiratory tract [4–7]. Therefore, numerous studies in recent years have focused on the formation of air pollution episodes in BTH [1, 8–14]. The air pollution is composed of multiple pollutants, which are mainly attributed to power plants, domestic pollutants, industry, and vehicle exhaust [9, 15–17]. Meteorological conditions are also important in modulating the distribution of atmospheric pollutants in the BTH [18–22]. Many studies have concluded that high relative humidity is conducive to secondary growth of pollutants, worsening air quality [23–25]. The convergence of pollutants is favored by calm or weak winds [26–29]. The formation of a temperature inversion is adverse to the dispersion of pollutants and exacerbates air pollution in BTH [23, 26–28]. There is a significant negative correlation between the concentration of pollutants and the height of the planetary boundary layer (PBL). A relatively low PBL height may aggravate air pollution [23, 26, 29]. Further, aerosols can alter the local spatial temperature distribution through a direct effect [30–32], thus modifying local atmospheric circulations. This in turn changes the distribution of aerosols, complicating the development of a pollution event [24, 26, 33–36]. From the perspective of dynamic mechanisms, Wu et al. [37] showed that strong and persistent sinking motion in the midlower troposphere over the BTH region can

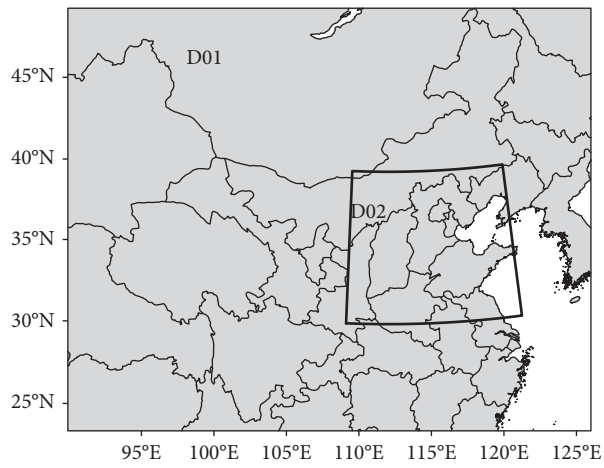

Figure 1: Domain of simulation.

reduce the PBL height and generate a temperature inversion, allowing air pollutants to accumulate in the lower PBL.

Regional transport also affects air pollution incidents. In addition to local emissions, the contribution of regional transport mainly depends on wind direction [19]. Taking Beijing as an example, southerly winds are more likely associated with severe air pollution than other wind directions because a portion of the pollutants and warm humid air can be carried from upwind areas to the city [18, 20, 23, 24, 27–29, 37–39]. With prevailing northerly winds, pollutants are exported from Beijing to its south [19, 38, 39]. On the contrary, in order to reduce pollution incidents, the Chinese government urges the BTH region and its neighboring area to adjust the energy structure in the way of closing down factories with high energy consumption and high pollution, promote the modification of desulphurization and denitrification, eliminate backward production capacity, and so on (http://www.hebqg.com/newsv.asp?nid=2025). Such kind of policy gives huge pressure to Hebei Province which relies much of its economic on the coal industry. Most regions in Hebei Province (especially the middle-south region) have to sacrifice a plenty of money in order to finish such kind of reformation of energy. A possible consequence is the stagnation of the economic development, as a result of which, a large number of workers will lose their jobs and local residents could hardly pass the cold winter without cheap heating system. For this reason, we hope to find the way which could guarantee the economic development and improve the air quality around Beijing-Tianjin with this hypothetical experiment. We conducted a hypothetical experiment using a WRF-Chem model to create a virtual terrain in Hebei Province. And trying to understand the impact of hypothetical topography on the distribution of pollutants in the BTH region when pollutants are based on the routine emissions. We investigated the heavy pollution event of 19 December 2016 to see whether virtual terrain can effectively block the transport of air pollutants. The formation mechanism of the events was analyzed. The spatial and temporal distribution and transmission regularity of air pollutants in the PBL were explored by setting up multiple virtual terrain experiments.

2. Model Configuration and Experimental Design

2.1. Model Configuration. The weather research and forecasting model coupled with chemistry (WRF-Chem, version 3.5.1) was used in the study, which simulates transport, diffusion, wet and dry deposition, emissions, aerosol gas-phase chemical reaction, liquid chemical reaction, photochemical reaction and radiation processes, and aerosols simultaneously with meteorological fields [40]. As shown in Figure 1, two nested domains (D01 and D02) were introduced to the model with horizontal resolutions 18 and 6 km, respectively. The D01 area covers most of mainland China and Mongolia and Korea, which could be used to analyze the large-scale circulation background of the pollution event. The D02 area covers BTH and its vicinity and was used to study air pollutant diffusion and transport in that region. To simulate the diffusion of air pollutants in the PBL more accurately, we increased the vertical resolution so that each domain had 42 vertical layers, extending from the surface to the 50 hPa level. The lowest 20 model sigma levels were 1.000, 0.9970, 0.9952, 0.9932, 0.9905, 0.9873, 0.9841, 0.9810, 0.9775, 0.9677, 0.9621, 0.9512, 0.9432, 0.9342, 0.9242, 0.9152, 0.9053, 0.8973, 0.8863, and 0.8783. Corresponding heights of each model layer were about 11.37, 29.58, 44.02, 61.91, 84.41, 108.89, 133.05, 158.47, 210.15, 270.39, 335.84, 411.49, 480.32, 558.03, 636.46, 715.28, 790.59, 871.40, 952.87, and 1034.84 m above the surface. The model used the Yonsei University PBL scheme [41], Lin microphysics scheme [42, 43], and rapid radiative transfer model for general circulation model longwave and shortwave radiation scheme [44] with aerosol direct effects. The gas-phase chemistry model was based on the Regional Acid Deposition Model version 2 [45], and the Modal Aerosol Dynamics Model for Europe/Secondary Organic Aerosol Model [46, 47] was used as the driver module for aerosol. Detailed model configurations and parameter options for physical and chemical processes are listed in Table 1. Meteorological initial and boundary conditions were from the $1^\circ \times 1^\circ$ National Centers for Environmental Prediction Final Analysis dataset (https://rda.ucar.edu/datasets/ds083.2). The monthly 2010 Multiresolution Emission Inventory for China (http://www.meicmodel.org/) was used for anthropogenic emissions. This emission inventory contains emissions of SO_2, NO_X, CO, NH_3, $PM_{2.5}$, PM_{10}, BC, OC, and nonmethane volatile organic compounds from five sectors (agriculture, industry, power plants, residential, and transportation), the diffusion (advection and convection), wet and dry deposition, and chemical reactions of which may produce secondary aerosols in WRF-Chem.

2.2. Experimental Design. Figure 2 shows terrain height in D02. The BTH region is surrounded by the Yanshan Mountains on the north, Taihang Mountains on the west, and Bohai Sea on the east. To the southeast is the relatively flat terrain of the North China Plain; only the central and southern parts of Shandong Province have hills. Neighboring cities south of Beijing are heavily industrialized. When there are

Table 1: CTL experiment mode settings.

Domain	D01	D02
Time step (s)	60	20
Horizontal resolution (km)	18	6
Domain size	168 × 168	181 × 175
Resolution of the terrain data	modis_30 s + 10 m	modis_30 s + 2 m
Vertical resolution	42	42
Boundary layer scheme	YSU	YSU
Cumulus parameterization scheme	Grell 3D	No
Microphysics scheme	Lin	Lin
Longwave radiation scheme	RRTMG	RRTMG
Shortwave radiation scheme	RRTMG	RRTMG
Chemical mechanism	RADM2	RADM2
Aerosols module	MADE/SORGAM	MADE/SORGAM
Aerosols feedback on radiation	On	On

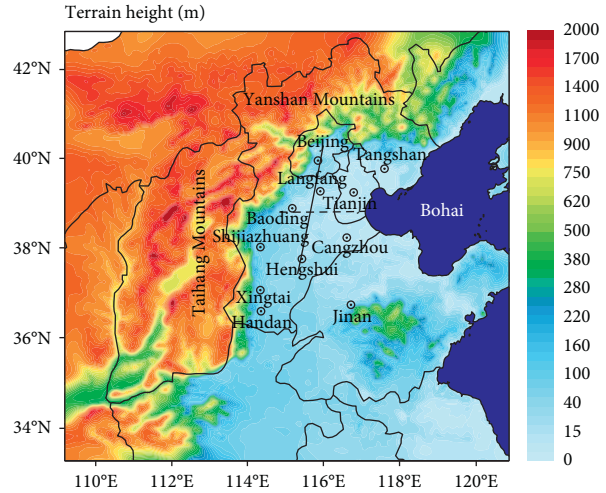

Figure 2: Topographic map of D02 (unit: m). Shading indicates terrain height, except for dark blue showing Bohai Sea. Black dotted line indicates location of hypothetical terrain, and solid black line indicates vertical cross section corresponding to Figure 7. Dotted circles indicate cities.

southerly winds over BTH, Beijing naturally becomes a pool for incoming pollutants because of its semibasin topography.

We simulated the heavy air pollution episode in BTH from 00:00 UTC on 16 December 2016 to 20 December (all subsequent time references are in UTC, which is late by Beijing time for 8 hours). We integrated over 96 h, the first 24 h of which were treated as the spin-up period. We mainly used a hypothetical terrain (HT) experiment to evaluate the transport of pollutants across the BTH region. First, a control experiment (CTL) was conducted using normal terrain to explore the spatiotemporal distribution of pollutants. Then, on the basis of the CTL, three groups of sensitivity experiments were run within the domain 115°E, 38.8°N to 117.54°E, 38.8°N, adding a hypothetical 400 meters (HGT400), 300 meters (HGT300), and 200 meters (HGT200) to the terrain. Corresponding locations are shown in Figure 2 by a black dotted line. Four experiments altering only terrain height were run to study the effects of the HT. Furthermore, we performed an experiment adding a hypothetical 500 meters to the terrain at the same location. However, its results revealed features similar to the HGT400 experiment. One possible reason is that contaminants are mainly diffused and transported below about 400 meters. Therefore, we only analyze the results of the CTL, HGT400, HGT300, and HGT200 simulations in this paper.

3. Model Evaluation

3.1. Surface Pressure Simulations. Figure 3 shows a comparison of observations and simulations for the large-scale background field. The simulated data are from the D01 region in the CTL run, and the observed data are from the Hong Kong Observatory surface weather map (http://www.envf.ust.hk/dataview/hkowc/current/). According to the observations, there was a high-pressure center of 1030 hPa over the Yangtze River Delta (YRD) region at 18:00 on 16 December 2016. Inner Mongolia was dominated by a cold high-pressure system with a central pressure of 1028 hPa. Pressure in the BTH region was lower than that in the two high-pressure areas. With the passage of time, both pressure systems over the YRD and Inner Mongolia moved eastward. By 00:00 on 18 December 2016, the YRD surface pressure system reached Japan and continued to move eastward. In spite of surface pressure in the BTH region increasing slightly, it was still intermediate to the two high-pressure systems. This caused a prevailing weak southerly wind southeast of BTH and a weak northerly wind to its northwest. Therefore, warm, moist air and pollutants may have been advected southeast of BTH, and cold, dry air transported to the northwest of BTH. By 00:00 on 19 December, pressure at BTH increased gradually, which is attributed to the cold high pressure over Inner Mongolia moving eastward slowly. At 18:00 on 16 December, the simulated high-pressure center of the YRD was similar to the observation. Although both the location of the low-pressure center around BTH and cold high-pressure center over Inner Mongolia are somewhat westward, simulated and observed values are nearly in agreement. At 00:00 on 18 December, simulated high-pressure system over South Korea was slightly west of the observed system, which may have been caused by the difference in size of the D01 area and synoptic chart. Fortunately, the performance for the BTH area between the two high-pressure systems was good. At 00:00 on 19 December, the simulated pressure over BTH was ~1026 hPa, 2 hPa lower than the observation. However, the simulations generally reproduced the large-scale background of the air pollution event.

3.2. Comparing Simulations with Observations. In this section, a comparison between the model results and observations for the time series of hourly relative humidity and temperature 2 m above the surface (RH2 and T2), surface $PM_{2.5}$, NO_2, and SO_2 concentration during from 04:00 on

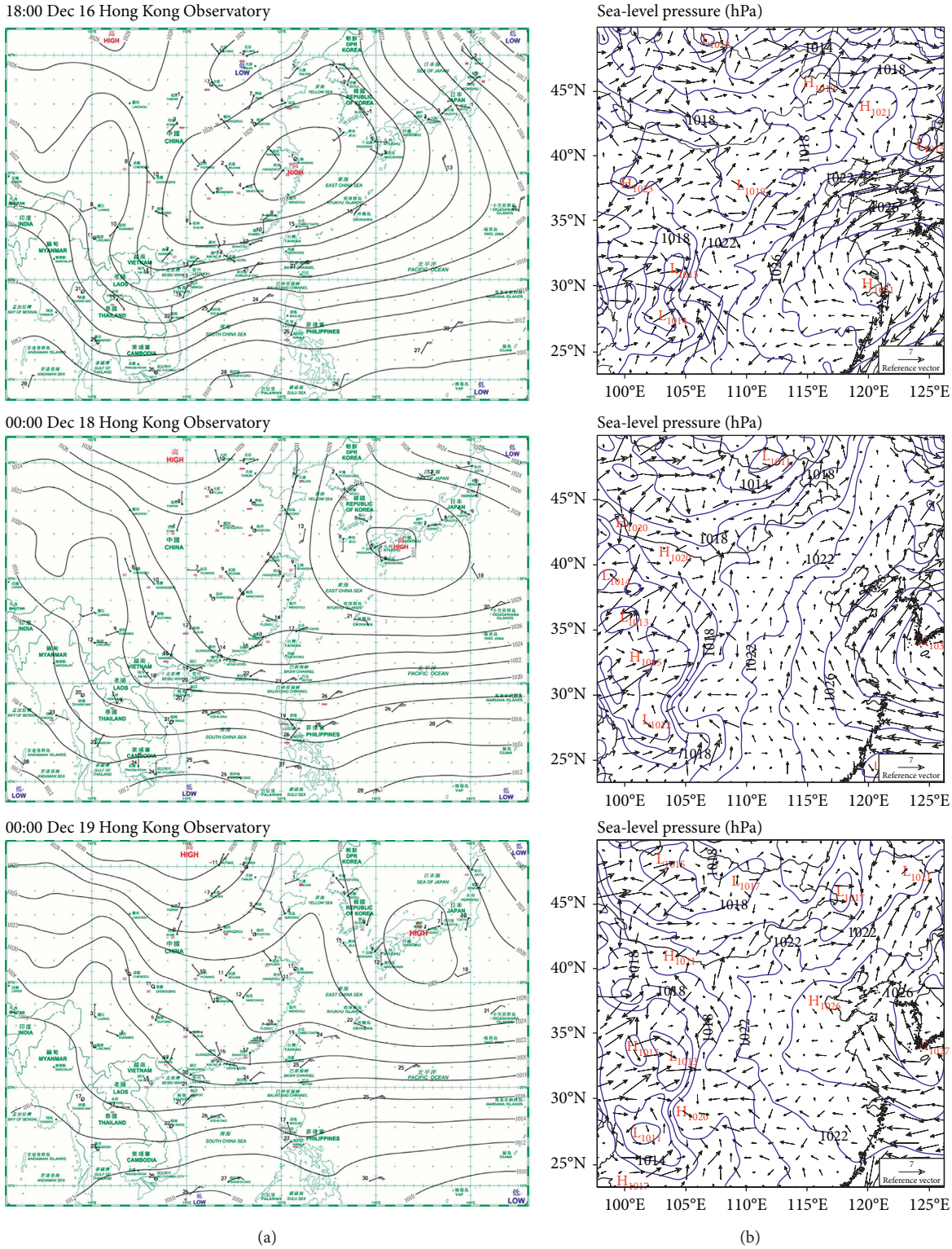

Figure 3: Surface weather chart from Hong Kong Observatory (a). For large-scale background field simulated in D01 (b), contour interval of sea-level pressure is 2 hPa, and black arrows show wind field 10 m above the surface; times are 18:00 on 16 December, 00:00 on 18 December, and 00:00 on 19 December 2016.

December 18 to 16:00 on December 19, 2016, is presented. To evaluate better the performance of the model in this study, Figure 4 is the time series of simulated and observed hourly averaged T2, RH2, $PM_{2.5}$, SO_2, and NO_2 at Beijing, Tianjin, Shijiazhuang, and Baoding, respectively. The corresponding statistical analysis results of the comparisons between simulated and observed are presented in Table 2. The observation data are from China's Ministry of

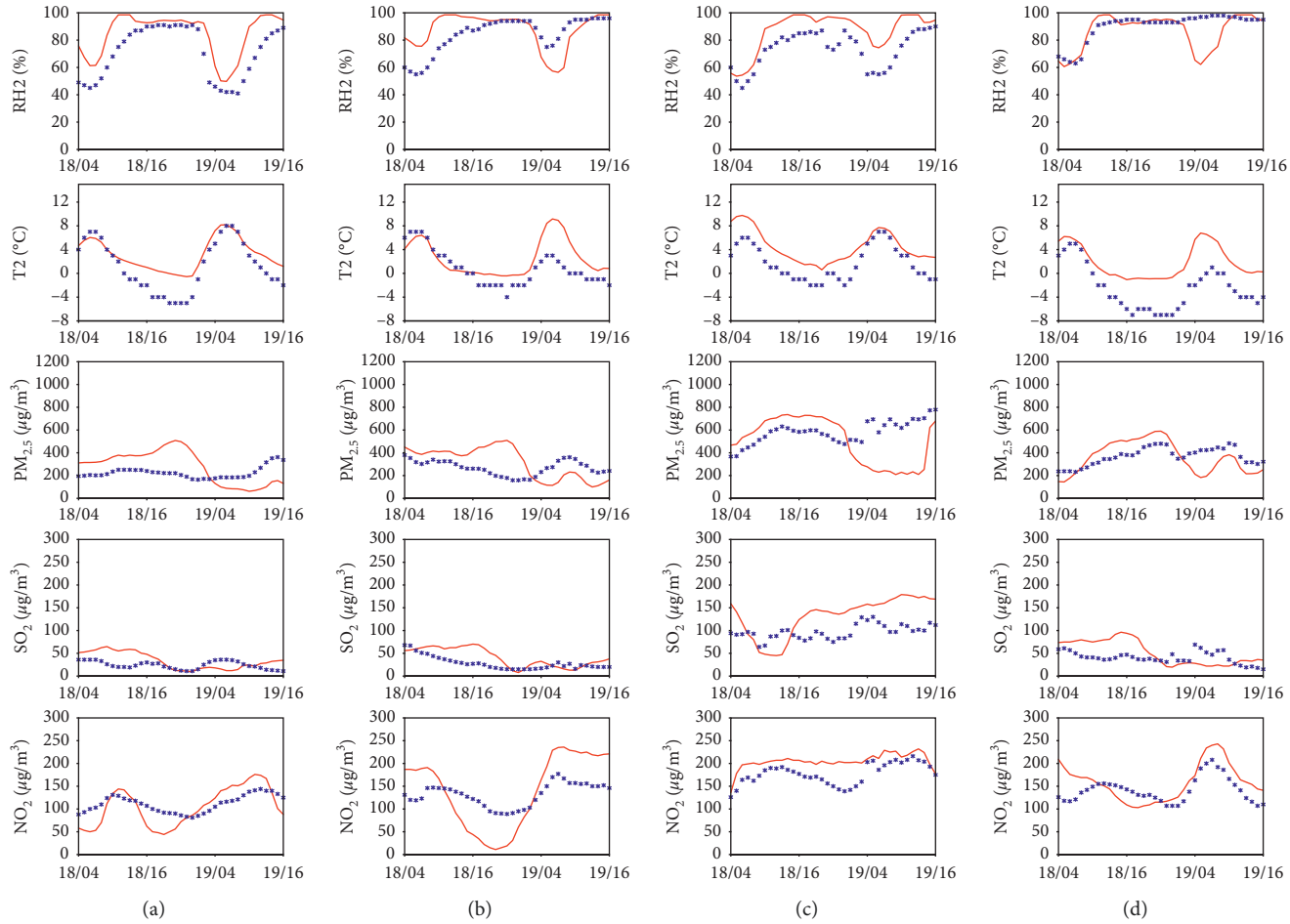

FIGURE 4: Simulated and observed hourly relative humidity and temperature 2 m above the surface (RH2, unit: %; T2, unit: ˚C), surface $PM_{2.5}$, NO_2, and SO_2 concentration (unit: $\mu g/m^3$) during from 04:00 on December 18 to 16:00 on December 19. The blue star indicates observed, and the red solid line indicates simulated. These four columns indicate (a) Beijing site, (b) Tianjin site, (c) Shijiazhuang site, and (d) Baoding site from left to right, respectively.

Environmental Protection and can be downloaded from the website https://www.zq12369.com/index.php. As illustrated in Figure 4 and Table 2, the model basically reproduces time and spatial distribution of these meteorological and chemical variables. For the RH2, the model can depict its temporal variation but slightly overestimates the values at the Beijing, Tianjin, and Shijiazhuang sites, and the corresponding mean bias (MB) are 13.99%, 4.04%, and 12.64%, respectively. Meanwhile, the observed RH2 are also high at the four sites, with observation mean (C_{OBS}) = 70.51 to 90.16%. The high RH2 may be conducive to secondary growth of air pollutants [23–25]. The observed T2 at the four sites are also reasonably reproduced by the model (root-mean-square error (RMSE) = 2.02 to 4.44 and normalized mean error (NME) = 0.01 to 0.03). However, the model overestimates the T2 values at the four sites, especially at the Baoding site where the MB is 3.38˚C. This may be attributed to the coarse resolution of the NCEP-FNL initial field. The initial and boundary meteorological conditions may also influence on the results of the simulations. In addition, the magnitudes and trends over time of the simulated $PM_{2.5}$, NO_2, and SO_2 are basically consistent with measurements (Figure 4). From Table 2, the model overestimates surface $PM_{2.5}$ concentration at the Beijing and Tianjin site (MB = 54.73 and 48.11 $\mu g/m^3$, respectively) and underestimates it at the Shijiazhuang and Baoding site (MB = −68.62 and −8.62 $\mu g/m^3$, respectively). In this air pollution period, surface $PM_{2.5}$ concentration is extremely high at the Shijiazhuang site, with model mean C_{MOD} and C_{OBS} as 521.95 and 581.57 $\mu g/m^3$, respectively. This may suggest more pollutants over the southern part of Hebei and transport of pollution to Beijing. In general, the model also reasonably reproduces the hourly variation of surface SO_2 concentration during from 04:00 on December 18 to 16:00 on December 19 2016 (RMSE = 20.63 to 50.70 and NME = 0.48 to 0.69). NO_2 is simulated very well in these three chemical variations, with MB = −5.95 to 27.76 $\mu g/m^3$ and normalized mean bias (NMB) = −0.05 to 0.16 at the four sites. Despite good simulation for these chemical variables, some deviations still exist. For example, the model underestimates the surface $PM_{2.5}$ concentration at the Shijiazhuang site during from 01:00 to 16:00 on December 19. This may be attributed to the uncertainties of emission inventory, coarse horizontal and vertical resolutions, inexact

Table 2: Performance statistics for meteorological and chemical variables from 04:00 on December 18 to 16:00 on December 18.

Variable	Site name	N^a	C_{OBS}	C_{MOD}	MB	RMSE	NMB	NME
RH2	Beijing	37	70.51	84.51	13.99	16.71	0.20	0.20
	Tianjin	37	88.14	84.11	4.04	14.10	0.05	0.12
	Shijiazhuang	37	73.38	87.02	12.64	15.34	0.19	0.19
	Baoding	37	90.16	86.48	−3.65	11.58	−0.04	0.08
T2	Beijing	37	1.19	3.15	1.96	2.66	1.64	0.02
	Tianjin	37	0.86	3.89	3.02	3.48	3.50	0.02
	Shijiazhuang	37	1.73	3.61	1.88	2.02	1.09	0.01
	Baoding	37	−2.54	0.83	3.38	4.44	−1.33	0.03
$PM_{2.5}$	Beijing	37	224.16	278.89	54.73	128.44	0.24	0.69
	Tianjin	37	267.86	315.97	48.11	122.31	0.18	0.53
	Shijiazhuang	37	581.57	512.95	−68.62	156.51	−0.15	0.37
	Baoding	37	369.27	360.65	−8.62	95.60	−0.02	0.28
SO_2	Beijing	37	24.05	33.83	9.77	20.63	0.41	0.69
	Tianjin	37	28.08	40.90	12.82	20.74	0.46	0.60
	Shijiazhuang	37	96.89	132.08	35.19	50.70	0.36	0.48
	Baoding	37	40.57	51.32	10.75	29.63	0.27	0.63
NO_2	Beijing	37	111.14	105.19	−5.95	30.38	−0.05	0.23
	Tianjin	37	131.32	139.68	8.35	60.22	0.06	0.42
	Shijiazhuang	37	177.24	205	27.76	31.96	0.16	0.15
	Baoding	37	141.08	158.27	17.19	34.12	0.12	0.21

N^a is the number of paired samples. C_{OBS} and C_{MOD} are the time series of the average of observation and model results. MB is the mean bias between the observation and model results. RMSE is the root-mean-square error of observation and model results. NMB is the normalized mean bias between the observation and model results. NME is the normalized mean error between the observation and model results.

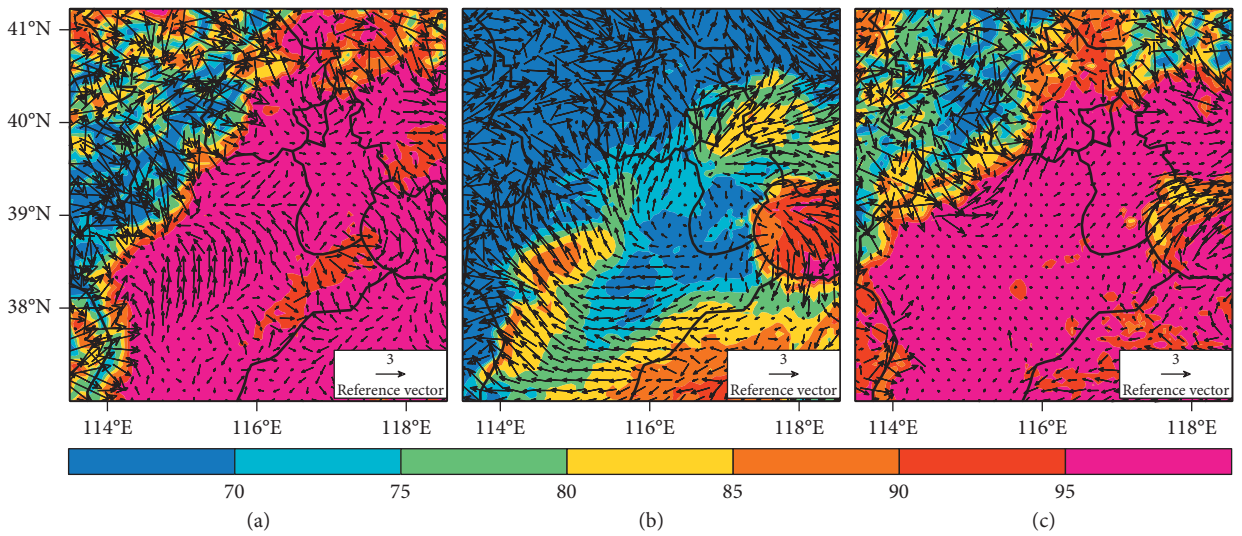

Figure 5: Wind speed 10 m above the surface and RH2 in CTL experiment. Black arrows show wind field (unit: m/s), and colors indicate RH2 (unit: %). Times are 22:00 on 18 December, 07:00 on 19 December, and 13:00 on 19 December 2016.

meteorological variables, and undiscovered processes of atmospheric chemistry [24]. Overall, however, the simulated results generally captured the heavy air pollution event that provides some reliability for the later sensitive experiments.

4. Analysis of Meteorological Elements

Figure 5(a) shows that RH2 exceeded 95% southeast of BTH but was low in the Taihang and Yanshan Mountains, which is attributable to the fact that water vapor content is less at higher altitudes and that a strong northwest wind was advecting dry and cold air over the two mountain ranges. Surface wind speed was <2 m/s on the BTH plain, except for the eastern Shijiazhuang area, where there was a strong southerly wind band that converged with the weak north wind over Baoding. Therefore, air pollution built southeast of BTH because of this meteorological situation (Figure 6(a)). The RH2 declined by 07:00 on 19 December, which can be attributed to a warming surface temperature caused by increasing solar radiation (Figure 5(b)). An anticyclone formed southeast of BTH, which reduced the water vapor content and air pollution through divergence, particularly to the south of Tianjin, Cangzhou, Hengshui, and Langfang

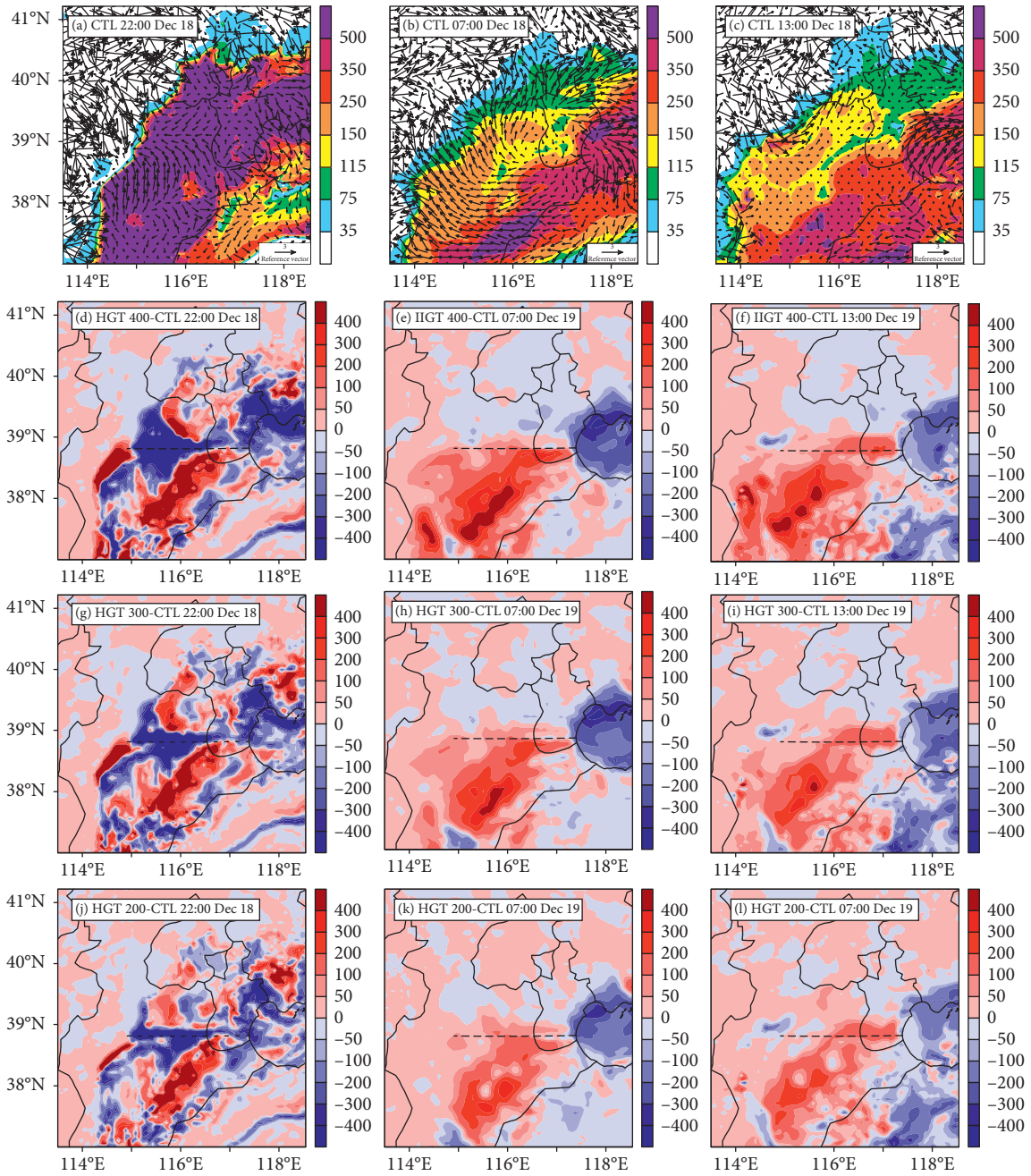

Figure 6: (a)–(c) $PM_{2.5}$ concentration horizontal distribution from CTL and difference between three sensitivity experiments and CTL; (d)–(f) HGT400-CTL; (g)–(i) HGT300-CTL; (j)–(l) HGT200-CTL (unit: $\mu g/m^3$). Black arrows show wind field, and black dotted line indicates location of the hypothetical terrain. Times are 22:00 on 18 December 2016, 07:00 on 19 December, and 13:00 on 19 December.

(Figures 5(b) and 6(b)). By 13:00 on 19 December (Figure 5(c)), there was a large area of calm or weak wind in the BTH region, and surface temperature was reduced by surface effective radiation, Hence, surface RH2 increased. Air pollution had not increased (Figure 6(c)), despite the high humidity and weak wind at BTH at this time. However, an hour later, concentrations of air pollutants gradually increased. This indicates that the increase of air pollution slightly lagged the weather conditions (figure not shown). Overall, a weak wind field is conducive to the persistence of water vapor and air pollutants. An accelerated formation of secondary aerosols may be attributed to hygroscopic contaminants in aqueous-phase chemical reactions under high humidity, consistent with other measurement and simulation studies [23–25, 27, 48].

5. Sensitivity Experiment Analysis

5.1. Horizontal Diffusion Characteristics. Some of the causes of the distribution and variation of air pollutants in the CTL run were discussed in Section 4. We now focus on the sensitivity experiments. We used the $PM_{2.5}$ concentration in the second layer of the model (~29.58 meters above the

surface) as the horizontal distribution of near-surface $PM_{2.5}$. Figure 6(d) shows an important phenomenon in which pollutant concentrations in southeastern Beijing, western Tianjin, north central Tangshan, northern Langfang, and southeastern HT had all increased, whereas there were decreases in southern Tangshan, eastern Tianjin, and over the Bohai Sea. The increases were mainly associated with the HT blocking effect, which reduced the spread of local pollutants. Decreases for the Tangshan and Tianjin coastal areas were also because of that effect, which prevented air pollutant transport from the southern HT to its north. However, the Bohai Sea area had reduced air pollutant concentrations. This may be attributed to the reduced pollutants in the Tangshan and Tianjin coastal areas, such that fewer pollutants were transported over the Bohai Sea, even with northwesterly and westerly winds. In addition, there was an extreme reduction of air pollution in the Baoding area, which may be attributed to the greatly enhanced convection near the HT region (Figure 7(a)). Thus, a large amount of contaminants was diffused at a high altitude, and they decreased dramatically at the surface. At 07:00 on 19 December (afternoon in Beijing) (Figure 6(b)), the contaminants decreased because of stronger wind speeds, warmer temperatures, and lower relative humidity. The pollutants concentrated south of the HT under the blocking effect, but north of the HT, there was not much decrease (Figure 6(e)). This may be explained by the few contaminants north of the HT at that time. The causes of the change in contaminants over the Bohai Sea are similar to 22:00 on 18 December. The Bohai Sea breeze direction gradually changed from south to southwest between 11:00 and 13:00 on 19 December, reducing pollutants over Cangzhou because they were transported over the sea (Figures 6(c)). Furthermore, the air pollutant concentration in southern HT increased, and the northern concentration decreased gradually with increase of HT height (Figures 6(e), 6(f), 6(h), 6(i), 6(k), and 6(l)). In addition, the HT clearly reduced the diffusion of local air pollutants, such as those in southern Beijing and western Langfang as seen in comparison to Figures 6(d), 6(g), and 6(j).

5.2. Vertical Profile Analysis. Figure 7 shows a vertical cross section of air pollutants. The black solid line in Figure 2 gives the horizontal location of the intercepted vertical cross section. For better comparison, all the intercepted times were the same at 22:00 on 18 December. To more clearly show variation of the vertical wind field, the vertical wind was exaggerated by 100 times. Figure 7(a) reveals that the wind direction was essentially horizontal. The maximum horizontal wind speed is 4.7 m/s and the minimum 0.002 m/s, which indicates that the stratification throughout the column was very stable. This was also a key indicator of air pollution formation. Temperature gradually decreased from south to north. In addition, a strong temperature inversion made it difficult for contaminants to disperse to high altitudes, so they mainly accumulated below 300 m. There was a relatively small amount of pollutants atop the inversion layer, which remained between 300 and 400 meters in height. From the HGT400 experiment (Figure 7(b)), substantial air pollution concentrated south of the HT and decreased steeply to its north because of the blocking effect. At the same time, the height of the inversion layer rose because of the HT, but pollutants remained below the top of temperature inversion. There was a large amount of contaminants diffused near the south side of the HT because of much stronger wind speeds and reverse flow. One can see that with the less weak wind speeds and reverse flow there with lower HT height (as compared with Figures 7(b)–7(d)), contaminants increased gradually there. There were two large-value centers on the north side of the HT, which were mainly responsible for local emissions. However, the lower HT height caused more pollutants from the south to cross the HT to the north side, increasing the two large-value centers.

5.3. Vertical Integration Concentration Analysis. The air pollutants were not only near the surface but also aloft, so we examined variation of the vertically integrated concentration. The equation for this concentration is

$$P_c = \sum_{i,j,k} P^*(i,j) * C(i,j,k) * \Delta\sigma(k), \quad (1)$$

where P^* is the pressure difference between the surface and model top, $C(i,j,k)$ is the pollution concentration, and $\Delta\sigma$ is the sigma level difference.

The distribution of $PM_{2.5}$ vertical concentration is basically consistent with that of the $PM_{2.5}$ concentration near the ground, as seen by comparing Figures 8(a)–8(c) with Figures 6(a)–6(c). This means that the pollutants were mainly near the ground and the concentration of pollutants at high altitude was low. At 22:00 on 18 December, southeastern Beijing, northwestern Tianjin, and northern Langfang air pollution decreased at high altitude for a HT of 400 meters, as seen by comparing Figure 8(d) with Figure 6(d). However, there were areas of strong air pollution at high altitude around Baoding, owing to strong horizontal and vertical wind speeds near the HT region, which may be attributed to the low resolution or model drawbacks as mentioned in Sections 5.1 and 5.2. In addition, from Figures 8(e), 8(f), 6(e), and 6(f), most of the pollutants concentrated near the surface during afternoon and night because of the blocking effect and stagnant meteorological conditions. Moreover, in contrast to Figures 8(d)–8(l), the lower the HT height, the more the contaminants were transported from south to north by crossing the HT.

6. Conclusions

We acquired encouraging results from the fully coupled WRF-Chem model, which was used to investigate the effects of HT height on air pollutant transport based on four experiments with differing HT heights. These experiments were designated CTL, HGT400, HGT300, and HGT200. The results show that warm, moist air and air pollutants were transported southeast of BTH because of high pressure in the northwestern Pacific, which increased the near-surface

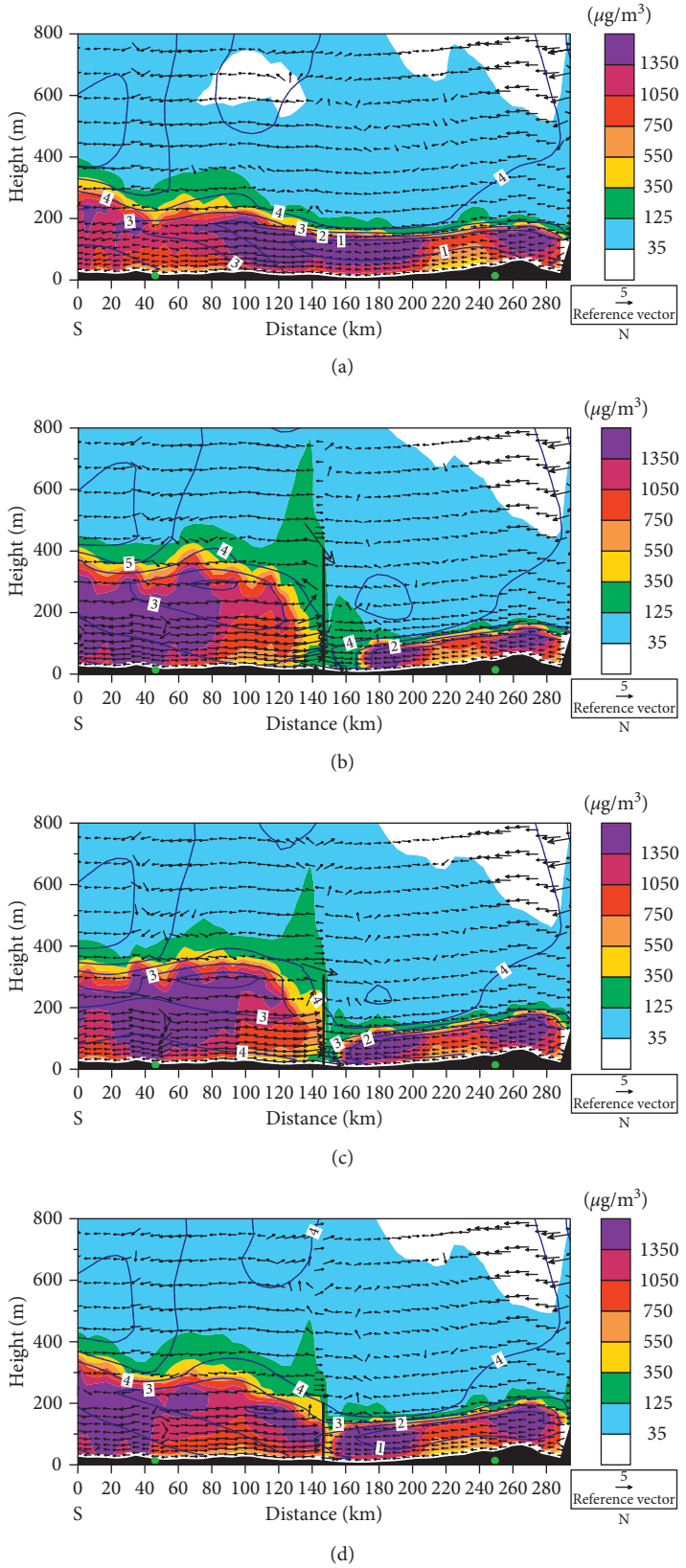

Figure 7: (a) Vertical cross section of $PM_{2.5}$ diffusion from CTL, and (b) differences of HGT400 and CTL simulations. (c) Differences of HGT300 and CTL simulations. (d) Differences of HGT200 and CTL simulations. Shading indicates $PM_{2.5}$ concentrations (unit: $\mu g/m^3$), contours show temperature (unit: °C), black arrows depict wind field, and green solid circles on the horizontal axis indicate locations of Hengshui and Beijing. Time is 22:00 on 18 December 2016.

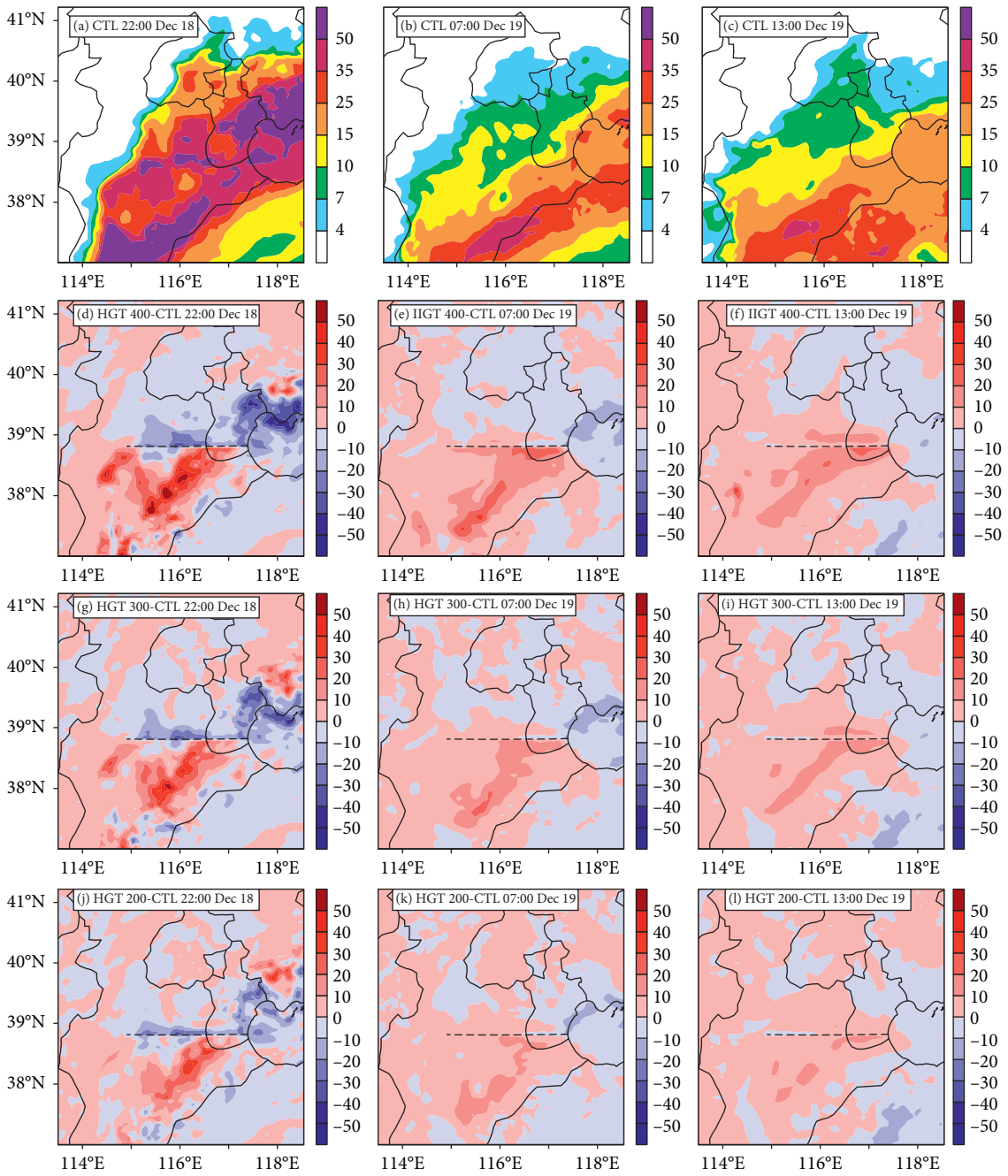

Figure 8: (a)–(c) Vertically integrated concentration of $PM_{2.5}$ from CTL. (d)–(f) Differences of HGT400 and CTL. (g)–(i) Differences of HGT300 and CTL. (j)–(l) Differences of HGT200 and CTL(unit: mm). Black dotted line indicates location of hypothetical terrain. Times are 22:00 on 18 December 2016, 07:00 on 19 December, and 13:00 on 19 December.

relative humidity and aggravated pollution. Stable weather conditions including a strong temperature inversion and weak wind are unfavorable for pollutant dispersion.

According to the four simulations, the pollutants were mainly diffused and transported below a height of 400 meters. The results also show the strong effect of HT on pollutant transport, which caused substantial pollutant concentration south of the HT. However, there was a slight decrease on the north side of the HT, which may have been caused by fewer total pollutants to the north of the HT. There were even some increases north of the HT because local emissions were obstructed by that terrain. Comparison of the simulations shows clearly that the greater the height of the HT below 400 meters, the stronger the blocking effect.

In essence, we still need to replace energy sources such as coal with clean energy to ensure the blue sky. This hypothetical experiment is impossible to achieve in real life, and we just hope that through hypothetical experiments to understand the distribution of pollutants in BTH area. The current experiments can be improved in several aspects. The model resolution was 6 km, which may be not adequate to resolve the PBL. The use of supercomputers should allow

simulations of air pollution events at greater resolution, possibly showing even greater sensitivity to the PBL. In this research, the observation data are primarily obtained at surface station only, and this may reduce the credibility of the simulations. Implementation of detailed PBL processes, accurate descriptions of pollutant transport, and using more observation data such as the radiosondes and satellite products will be the next step toward improvement of simulation by WRF-Chem.

Data Availability

The National Centers for Environmental Prediction Final Global Tropospheric Analysis (NCEP-FNL) data were taken from https://rda.ucar.edu/datasets/ds083.2. The data used to support the findings of this study are available from the corresponding author upon request.

Conflicts of Interest

The authors declare that they have no conflicts of interest.

Acknowledgments

The authors were supported by the National Program for Key Basic Research Projects of China (973) (Grant no. 2014CB953904), Natural Science Foundation of Guangdong Province (2015A030311026), National Natural Science Foundation of China (NSFC) (Grant nos. 41275145 and 41705117), and Guangzhou Science and Technology Plan (201707010088). The authors thank the Special Program for Applied Research on Super Computation of the NSFC-Guangdong Joint Fund (second phase) under Grant no. U1501501. The authors are grateful to the NCAR Mesoscale and Microscale Meteorology Division for making the WRF-Chem model available at http://www.mmm.ucar.edu/wrf/users.

References

[1] Y. C. Miao, X. M. Hu, S. H. Liu et al., "Seasonal variation of local atmospheric circulations and boundary layer structure in the Beijing-Tianjin-Hebei region and implications for air quality," *Journal of Advances in Modeling Earth Systems*, vol. 7, no. 4, pp. 1602–1626, 2015.

[2] A. V. Donkelaar, R. V. Martin, M. Brauer et al., "Global estimates of ambient fine particulate matter concentrations from satellite-based aerosol optical depth: development and application," *Environmental Health Perspectives*, vol. 118, no. 6, pp. 847–855, 2010.

[3] J. Z. Ma, X. B. Xu, C. S. Zhao, and P. Yan, "A review of atmospheric chemistry research in China: photochemical smog, haze pollution, and gas-aerosol interactions," *Advances in Atmospheric Sciences*, vol. 29, no. 5, pp. 1006–1026, 2012.

[4] P. J. Adams, J. H. Seinfeld, D. Koch, L. Mickley, and D. Jacob, "General circulation assessment of direct radiative forcing by the sulphate-nitrate-ammonium-water inorganic aerosol system," *Journal of Geophysical Research*, vol. 106, no. 1, pp. 1097–1111, 2001.

[5] M. Z. Jacobson, "Global direct radiative forcing due to multicomponent anthropogenic and natural aerosols," *Journal of Geophysical Research*, vol. 106, no. 2, pp. 1551–1568, 2001.

[6] T. Elias, M. Haeffelin, P. Drobinski, and M. Colomb, "Particulate contribution to extinction of visible radiation: pollution, haze, and fog," *Atmospheric Research*, vol. 92, no. 4, pp. 443–454, 2009.

[7] The World Health Organization (WHO), *7 Million Premature Deaths Annually Linked to Air Pollution*, 2014, http://www.who.int/mediacentre/news/releases/2014/air-pollution/en/.

[8] R.J. Huang, S. Szidat, I. Haddad et al., "High secondary aerosol contribution to particulate pollution during haze events in China," *Nature*, vol. 514, pp. 218–222, 2014.

[9] J. Liu, D. L. Mauzerall, Q. Chen et al., "Air pollutant emissions from Chinese households: a major and underappreciated ambient pollution source," *Proceedings of the National Academy of Sciences of the United States of America*, vol. 113, no. 28, pp. 7756–7761, 2016.

[10] X. Zhao, X. Zhang, X. Xu, J. Xu, W. Meng, and W. Pu, "Seasonal and diurnal variations of ambient $PM_{2.5}$ concentration in urban and rural environments in Beijing," *Atmospheric Environment*, vol. 43, no. 18, pp. 2893–2900, 2009.

[11] G. Tian, Z. Qiao, and X. Xu, "Characteristics of particulate matter (PM10) and its relationship with meteorological factors during 2001-2012 in Beijing," *Environmental Pollution*, vol. 192, pp. 266–274, 2014.

[12] Z. Liu, B. Hu, D. Ji, Y. Wang, M. Wang, and Y. Wang, "Diurnal and seasonal variation of the $PM_{2.5}$, apparent particle density in Beijing, China," *Atmospheric Environment*, vol. 120, pp. 328–338, 2015.

[13] X. An, T. Zhu, Z. Wang, Z. Li, and Y. Wang, "A modeling analysis of a heavy air pollution episode occurred in Beijing," *Atmospheric Chemistry and Physics*, vol. 7, no. 12, pp. 3103–3114, 2007.

[14] L. Wang, J. Xu, J. Yang et al., "Understanding haze pollution over the southern Hebei area of China using the CMAQ model," *Atmospheric Environment*, vol. 56, no. 5, pp. 69–79, 2012.

[15] R. Wu, J. Li, Y. Hao, Y. Li, L. Zeng, and S. Xie, "Evolution process and sources of ambient volatile organic compounds during a severe haze event in Beijing, China," *Science of the Total Environment*, vol. 560-561, pp. 62–72, 2016.

[16] G. Wang, S. Cheng, W. Wei et al., "Characteristics and emission-reduction measures evaluation of $PM_{2.5}$ during the two major events: APEC and Parade," *Science of the Total Environment*, vol. 595, pp. 81–92, 2017.

[17] Y. Wang, Y. Xue, H. Tian et al., "Effectiveness of temporary control measures for lowering $PM_{2.5}$ pollution in Beijing and the implications," *Atmospheric Environment*, vol. 157, pp. 75–83, 2017.

[18] Y. Sun, C. Chen, Y. Zhang et al., "Rapid formation and evolution of an extreme haze episode in northern china during winter 2015," *Scientific Reports*, vol. 6, no. 1, pp. 27151–27159, 2016.

[19] J. Wang, M. Zhang, X. Bai et al., "Large-scale transport of $PM_{2.5}$ in the lower troposphere during winter cold surges in China," *Scientific Reports*, vol. 7, no. 1, pp. 13238–13247, 2017.

[20] G. J. Zheng, F. K. Duan, H. Su et al., "Exploring the severe winter haze in Beijing: the impact of synoptic weather, regional transport and heterogeneous reactions," *Atmospheric Chemistry and Physics*, vol. 15, no. 6, pp. 2969–2983, 2015.

[21] L. Wang, N. Zhang, Z. Liu, Y. Sun, D. Ji, and Y. Wang, "The influence of climate factors, meteorological conditions, and boundary-layer structure on severe haze pollution in the Beijing-Tianjin-Hebei region during January 2013," *Advances in Meteorology*, vol. 2014, Article ID 685971, 14 pages, 2014.

[22] Y. Wang, L. Wang, G. Zhao et al., "Analysis of different-scales circulation patterns and boundary layer structure of $PM_{2.5SO}$ heavy pollutions in Beijing during winter," *Climatic Environmental Research*, vol. 19, no. 2, pp. 173–184, 2014, in Chinese.

[23] Y. Yang, X. Liu, Y. Qu et al., "Formation mechanism of continuous extreme haze episodes in the megacity Beijing, China, in January 2013," *Atmospheric Research*, vol. 155, pp. 192–203, 2015.

[24] M. Gao, G. R. Carmichael, Y. Wang et al., "Modeling study of the 2010 regional haze event in the North China Plain," *Atmospheric Chemistry and Physics*, vol. 15, no. 16, pp. 22781–22822, 2016.

[25] M. Wang, C. Cao, G. Li, and R. P. Singh, "Analysis of a severe prolonged regional haze episode in the Yangtze River Delta, China," *Atmospheric Environment*, vol. 102, pp. 112–121, 2015.

[26] J. Wang, S. Wang, J. Jiang et al., "Impact of aerosol-meteorology interactions on fine particle pollution during China's severe haze episode in January 2013," *Environmental Research Letters*, vol. 9, no. 9, pp. 1–7, 2014.

[27] X. J. Zhao, P. S. Zhao, J. Xu, and W. Meng, "Analysis of a winter regional haze event and its formation mechanism in the North China Plain," *Atmospheric Chemistry and Physics*, vol. 13, no. 11, pp. 5685–5696, 2013.

[28] L. Zhang, T. Wang, M. Lv, and Q. Zhang, "On the severe haze in Beijing during January 2013: unraveling the effects of meteorological anomalies with WRF-Chem," *Atmospheric Environment*, vol. 104, pp. 11–22, 2015.

[29] H. He, X. Tie, Q. Zhang et al., "Analysis of the causes of heavy aerosol pollution in Beijing, China: a case study with the WRF-Chem model," *Particuology*, vol. 20, no. 3, pp. 32–40, 2015.

[30] M. A. Atwater, "Planetary albedo changes due to aerosols," *Science*, vol. 170, no. 3953, pp. 64–66, 1970.

[31] I. N. Sokolik and O. B. Toon, "Direct radiative forcing by airborne mineral aerosols," *Journal of Aerosol Science*, vol. 27, no. 6584, pp. 11-12, 1996.

[32] H. Yu, Y. J. Kaufman, M. Chin, and G. Feingold, "A review of measurement-based assessments of the aerosol direct radiative effect and forcing," *Atmospheric Chemistry and Physics*, vol. 6, no. 11, pp. 613–666, 2006.

[33] Y. Miao, S. Liu, Y. Zheng, and S. Wang, "Modeling the feedback between aerosol and boundary layer processes: a case study in Beijing, China," *Environmental Science and Pollution Research*, vol. 23, no. 4, pp. 3342–3357, 2016.

[34] Y. Miao, S. Liu, Y. Zheng et al., "Numerical study of the effects of local atmospheric circulations on a pollution event over Beijing-Tianjin-Hebei, China," *Journal of Environmental Sciences*, vol. 30, no. 4, pp. 9–20, 2015.

[35] Z. F. Wang, J. Li, Z. Wang et al., "Modeling study of regional severe hazes over mid-eastern China in January 2013 and its implications on pollution prevention and control," *Science China: Earth Sciences*, vol. 57, no. 1, pp. 3–13, 2014.

[36] Y. Gao, M. Zhang, Z. Liu et al., "Modeling the feedback between aerosol and meteorological variables in the atmospheric boundary layer during a severe fog-haze event over the North China Plain," *Atmospheric Chemistry and Physics*, vol. 15, no. 8, pp. 4279–4295, 2015.

[37] P. Wu, Y. Ding, and Y. Liu, "Atmospheric circulation and dynamic mechanism for persistent haze events in the Beijing-Tianjin-Hebei region," *Advances in Atmospheric Sciences*, vol. 34, no. 4, pp. 429–440, 2017.

[38] J. Li and Z. Han, "A modeling study of severe winter haze events in Beijing and its neighboring regions," *Atmospheric Research*, vol. 170, pp. 87–97, 2016.

[39] S. Guo, M. Hu, M. Zamora et al., "Elucidating severe urban haze formation in China," *Proceedings of the National Academy of Sciences of the United States of America*, vol. 111, no. 49, pp. 17373–17378, 2014.

[40] G. A. Grell, S. E. Pechham, R. Schmitz et al., "Fully coupled "online" chemistry within the WRF model," *Atmospheric Environment*, vol. 39, no. 37, pp. 6957–6975, 2005.

[41] S. Y. Hong, Y. Noh, and J. Dudhia, "A new vertical diffusion package with an explicit treatment of entrainment processes," *Monthly Weather Review*, vol. 134, no. 9, pp. 2318–2341, 2006.

[42] Y. L. Lin, R. D. Farley, and H. D. Orvilie, "Bulk parameterization of the snow field in a cloud model," *Journal of Climate and Applied Meteorology*, vol. 22, no. 6, pp. 1065–1092, 1983.

[43] S. Y. Hong, J. Dudhia, and S. H. Chen, "A revised approach to ice microphysical processes for the bulk parameterization of clouds and precipitation," *Monthly Weather Review*, vol. 132, no. 1, pp. 103–120, 2004.

[44] M. J. Iacono, J. S. Delamere, E. J. Mlawer, M. W. Shephard, S. A. Clough, and W. D. Collins, "Radiative forcing by long-lived greenhouse gases: calculations with the AER radiative transfer models," *Journal of Geophysical Research*, vol. 113, no. 13, article D13103, 2008.

[45] W. R. Stockwell, P. Middleton, J. S. Chang, and X. Tang, "The second generation regional acid deposition model chemical mechanism for regional air quality modeling," *Journal of Geophysical Research*, vol. 95, no. 10, pp. 16343–16367, 1990.

[46] I. J. Ackermann, H. Hass, M. Memmesheimer, A. Ebel, F. S. Binkowski, and U. Shankar, "Modal aerosol dynamics model for Europe: development and first applications," *Atmospheric Environment*, vol. 32, no. 17, pp. 2981–2999, 1998.

[47] B. Schell, I. J. Ackermann, H. Hass, F. S. Binkowski, and A. Ebel, "Modeling the formation of secondary organic aerosol within a comprehensive air quality model system," *Journal of Geophysical Research: Atmospheres*, vol. 106, no. 22, pp. 28275–28293, 2001.

[48] F. Xiao, S. Wang, C. Xing, S. Cai, X. Jia, and J. Hao, "Modeling analysis of secondary inorganic aerosols over China: pollution characteristics, and meteorological and dust impacts," *Scientific Reports*, vol. 6, no. 1, pp. 35992–35998, 2016.